



Article

Ammonium Ion Enhanced V₂O₅-WO₃/TiO₂ Catalysts for Selective Catalytic Reduction with Ammonia

Min Seong Lee^{1,2,†}, Sun-I Kim^{1,†}, Bora Jeong¹, Jin-Woo Park^{2,3}, Taehyo Kim¹, Jung Woo Lee² , Gibum Kwon^{4,*} and Duck Hyun Lee^{1,*}

¹ Green Materials & Processes R&D Group, Korea Institute of Industrial Technology, Ulsan 44413, Korea; qneh5@kitech.re.kr (M.S.L.); sunikim@kitech.re.kr (S.-I.K.); bora1106@kitech.re.kr (B.J.); thkim0215@kitech.re.kr (T.K.)

² Department of Materials Science & Engineering, Pusan National University, Busan 46241, Korea; parkjw@nanoin.com (J.-W.P.); jungwoolee@pusan.ac.kr (J.W.L.)

³ NANO. Co., Ltd., Sangju 37257, Korea

⁴ Department of Mechanical Engineering, University of Kansas, Lawrence, KS 66045, USA

* Correspondence: gbkwon@ku.edu (G.K.); dulee@kitech.re.kr (D.H.L.); Tel.: +1-785-864-1086 (G.K.); +82-52-980-6709 (D.H.L.); Fax: +82-52-980-6669 (D.H.L.)

† Both authors contributed equally to this work.

Abstract: Selective catalytic reduction (SCR) is the most efficient NO_x removal technology, and the vanadium-based catalyst is mainly used in SCR technology. The vanadium-based catalyst showed higher NO_x removal performance in the high-temperature range but catalytic efficiency decreased at lower temperatures, following exposure to SO_x because of the generation of ammonium sulfate on the catalyst surface. To overcome these limitations, we coated an NH₄⁺ layer on a vanadium-based catalyst. After silane coating the V₂O₅-WO₃/TiO₂ catalyst by vapor evaporation, the silanized catalyst was heat treated under NH₃ gas. By decomposing the silane on the surface, an NH₄⁺ layer was formed on the catalyst surface through a substitution reaction. We observed high NO_x removal efficiency over a wide temperature range by coating an NH₄⁺ layer on a vanadium-based catalyst. This layer shows high proton conductivity, which leads to the reduction of vanadium oxides and tungsten oxide; additionally, the NO_x removal performance was improved over a wide temperature range. These findings provide a new method to develop SCR catalyst with high efficiency at a wide temperature range.

Keywords: selective catalytic reduction; V-based catalyst; NO_x removal efficiency; silane; ammonium



Citation: Lee, M.S.; Kim, S.-I.; Jeong, B.; Park, J.-W.; Kim, T.; Lee, J.W.; Kwon, G.; Lee, D.H. Ammonium Ion Enhanced V₂O₅-WO₃/TiO₂ Catalysts for Selective Catalytic Reduction with Ammonia. *Nanomaterials* **2021**, *11*, 2677. <https://doi.org/10.3390/nano11102677>

Academic Editor: Maria Filipa Ribeiro

Received: 31 August 2021

Accepted: 5 October 2021

Published: 12 October 2021

Publisher's Note: MDPI stays neutral with regard to jurisdictional claims in published maps and institutional affiliations.



Copyright: © 2021 by the authors. Licensee MDPI, Basel, Switzerland. This article is an open access article distributed under the terms and conditions of the Creative Commons Attribution (CC BY) license (<https://creativecommons.org/licenses/by/4.0/>).

1. Introduction

Most energy is generated through the combustion of fossil fuels, which causes air pollution by emitting toxic pollutants, such as NO_x, particulate matter, SO_x, and CO [1,2]. Nitrogen oxides (NO, NO₂, and N₂O) are the most representative air pollutants because they are major causes of acid rain, photochemical smog, ozone depletion, and global warming [3–5]. NO_x is emitted by automobiles, power stations, industrial heaters, and non-road vehicles. To reduce this form of pollution, NO_x removal technologies must be developed. Many technologies have been developed to control NO_x emissions, such as selective catalytic reduction (SCR), non-selective catalytic reduction (NSCR), and selective non-catalytic reduction (SNCR). Selective catalytic reduction (SCR), the most efficient NO_x removal technology, selectively converts NO_x in fuel gas into N₂ and H₂O. Compared with other technologies, such as non-selective catalytic reduction (NSCR) and selective non-catalytic reduction (SNCR), SCR shows a high NO_x removal efficiency and no secondary pollutant emission and can be operated in the temperature range of 100–300 °C [4].

The V₂O₅-WO₃/TiO₂ catalyst has been commercially applied for SCR of NO_x with NH₃ because of its good thermal stability, N₂ selectivity, and low SO₂ oxidation activity

for conversion to SO_3 [6]. However, this catalyst shows high NO_x removal performance only in the temperature range of 300–400 °C, and performance decreases at temperatures below 300 °C [7,8]. Therefore, many studies have been conducted to develop catalysts that function over a wide temperature range such as 200–420 °C. Djerad et al. increased the loading of V_2O_5 in WO_3/TiO_2 catalysts to improve NO_x removal efficiency at lower temperatures [9,10]. A higher V_2O_5 content leads to increased catalytic activity but decreased N_2 selectivity and a narrow activation temperature range. Other researchers modified catalysts using transition metal oxides (Co, Mn, Ce, Cu, etc.) and rare-earth oxides (Eu, Sm, Nd, and Ho) [3,11–19]. For example, Wang et al. investigated the effect of adding Cu to a $\text{V}_2\text{O}_5\text{-WO}_3/\text{TiO}_2$ catalyst on low-temperature $\text{NH}_3\text{-SCR}$ performance [20]. The added Cu oxides improved the catalytic activity of V_2O_5 by increasing the redox property of V_2O_5 ($\text{Cu}^{2+} + \text{V}^{4+} \rightleftharpoons \text{V}^{5+} + \text{Cu}^+$), leading to a fast SCR reaction. Guo et al. modified Nd on MnOx catalysts to improve NH_3 SCR performance [21]. The catalytic activity and N_2 selectivity were enhanced by doping MnOx with an Nd catalyst. Although catalytic activity was improved at low temperatures (>300 °C), the catalytic performance decreased at temperatures above 400 °C. Therefore, covering a wide window temperature by modifying only the catalyst remains challenging. Another method for improving NO_x removal technology at wide temperature ranges (200–420 °C) involves applying ammonium nitrate (NH_4NO_3) on the catalysts [22–24]. Chae et al. enhanced the catalytic performance of SCR of NO_x at temperatures below 300 °C by injecting liquid ammonium nitrate on a $\text{V}_2\text{O}_5\text{-Sb}_2\text{O}_3/\text{TiO}_2$ catalyst. The injected ammonium nitrate led to a fast SCR and prevented the formation of ammonia bisulfate on the catalyst surface and catalytic deactivation by SO_2 at temperatures below 300 °C.

In this study, we enhanced the NO_x removal efficiency and N_2 selectivity over a wide temperature range of 200–420 °C by improving the catalytic activity at temperatures below 300 °C. The catalyst surface was coated with a silane layer, and the silane molecules evaporated with heat treatment at 500 °C in NH_3 environment. The resulting catalyst surface was substituted with NH_4^+ layers present, and the NH_4^+ layers formed on the surface of the $\text{V}_2\text{O}_5\text{-WO}_3/\text{TiO}_2$ catalyst increased NO_x removal efficiency at low temperatures (200–250 °C).

2. Materials and Methods

2.1. Catalyst Preparation

The NH_4^+ -coated $\text{V}_2\text{O}_5\text{-WO}_3/\text{TiO}_2$ catalyst was prepared in three steps: first, $\text{V}_2\text{O}_5\text{-WO}_3/\text{TiO}_2$ was synthesized by the impregnation method, and then, the catalyst underwent vapor phase silane treatment at 180 °C for 1 h. Finally, the silanized $\text{V}_2\text{O}_5\text{-WO}_3/\text{TiO}_2$ catalysts were heat treated under NH_3 gas with N_2 gas.

To synthesize 2 wt.% V_2O_5 – 10 wt.% WO_3/TiO_2 , 8.800 g of TiO_2 powder (8.800 g, NANO Co., Ltd., Seoul, Korea, NT-01), 0.256 g of NH_4VO_3 (Sigma-Aldrich, St. Louis, MO, USA, 99.99%), 1.062 g of $(\text{NH}_4)_6\text{H}_2\text{W}_{12}\text{O}_{40} \times \text{H}_2\text{O}$ (Sigma-Aldrich, St. Louis, MO, USA, 99.99%), and 0.386 g of oxalic acid were mixed with 100 mL of deionized water and stirred for 2 h. The solution in the mixture was evaporated at 85 °C in an oil bath for impregnation of V and W atoms followed by drying in an oven at 110 °C for 12 h. The dried powder was placed in a furnace and calcinated at 500 °C under atmospheric pressure.

Vapor phase silanization was conducted. First, the catalyst was cleaned by ozone treatment to remove any impurities and to increase hydroxyl species on the surface. The catalyst was placed in a sealed Teflon jar with 1.0 mL of Trichloro (1H, 1H, 2H, 2H-perfluorooctyl) silane (Sigma-Aldrich, 97%). The jar was subjected to 180 °C to vary the time. To coat the NH_4^+ on the catalyst, the silanized $\text{V}_2\text{O}_5\text{-WO}_3/\text{TiO}_2$ catalyst underwent heat treatment at 500 °C for 2 h upon purging a of NH_3 gas (300 ppm) for 2 h.

To observe the effect of the NH_4^+ layer on the commercial catalyst, we prepared commercial plate-type monoliths. The catalyst, consisting of V_2O_5 , MoO_3 , and TiO_2 , was pasted on the wall of the plate, which had dimensions of 1 mm \times 34 mm \times 187 mm, and an

NH₄⁺ layer coating was performed. After silane coating by vapor deposition, the catalysts were heat treated at 500 °C under 300 ppm NH₃ gas with N₂ gas for 2 h.

2.2. Catalyst Characterization

The effect of each preparation step on the catalyst morphology was investigated by field emission scanning electron microscopy (Hitachi, Tokyo, Japan, SU8020) at an accelerating voltage of 15.0 kV. The surface properties were determined by measuring the water contact angle using the static sessile drop method with a Contact angle analyzer (Phoenix 300, SEO, Suwon, Korea). The contact angle of the prepared catalysts (thickness = about 0.2 cm) was measured within 10 s after dropping water.

The crystallinity of and impurities in the catalysts were analyzed using X-ray diffraction (XRD, Rigaku, Tokyo, Japan, Ultima IV) with Cu K α ($\lambda = 0.15406$ nm) radiation in the 2θ range of 10° to 80° at a scan rate of 1°/min. The Si and N elements in the catalysts were measured by X-ray photoelectron spectroscopy (XPS; Thermo VG Scientific, Waltham, MA, USA, K Alpha+) with Al K α radiation; the binding energy of C1s was normalized to 284.8 eV. Fourier transform infrared spectroscopy (FT-IR, Varian Medical Systems, Palo Alto, CA, USA, 670 FTIR) was carried out over a wavelength range of 400–4000 cm⁻¹.

H₂-temperature-programmed reduction was carried out using an AutoChem II 2920 (Micromeritics Instrument Corp., Norcross, GA, USA). The samples were exposed to a current of 10% H₂/Ar and measured in the 200–900 °C temperature range.

2.3. Catalytic Activity Measurement

The NO_x removal efficiency of the catalysts was evaluated in a fixed-bed reactor under high atmospheric pressure, with the sample placed on a stainless-steel tube and analyzed using a powder catalyst. The analysis temperature was varied from 150 °C to 420 °C, and the reactive gas was composed of 300 ppm NO_x, 300 ppm NH₃ (NH₃/NO_x = 1.0), 300 ppm SO₂, and 5 vol.% of O₂, with a N₂ balance under a total flow rate of 500 sccm. The powder catalyst (0.35 g) was tested, and the gas hourly space velocity was set at 60,000 h⁻¹. Plate-type commercial catalysts were evaluated in a microreactor. The analysis temperature was varied from 200 °C to 450 °C, and the reactive gas was composed of 240 ppm NO_x, 288 ppm NH₃ (NH₃/NO_x = 1.2), 600 ppm SO₂, and 3 vol.% of O₂, with a N₂ balance under a total flow rate of 1.2 m³/h; the area velocity was set to 25 m/h. The reactive gas concentration was determined by FT-IR (Gaset, Vantaa, Finland, CX-4000) and gas analysis spectrometry (DSMXT, Heidelberg, Germany). NO_x removal efficiency and N₂ selectivity were calculated according to Equations (1) and (2), respectively.

$$\text{NO}_x \text{ removal efficiency (\%)} = \frac{\text{NO}_x \text{ inlet} - \text{NO}_x \text{ outlet}}{\text{NO}_x \text{ inlet}} \times 100, \quad (1)$$

$$\text{N}_2 \text{ selectivity (\%)} = \frac{\text{NO}_{\text{inlet}} - \text{NO}_{\text{outlet}} - \text{NO}_2 \text{ outlet} - \text{N}_2\text{O}_{\text{outlet}}}{\text{NO}_{\text{inlet}} - \text{NO}_{\text{outlet}}} \times 100, \quad (2)$$

3. Results

Figure 1 illustrates the process of producing the NH₄⁺ layer on the V₂O₅-WO₃/TiO₂ catalysts. The surface of the synthesized V₂O₅-WO₃/TiO₂ catalysts is hydrophilic because of the presence of numerous oxygen groups. After the catalysts were silanized at 180 °C for 1 h, the surface properties became hydrophobic because of the hydrophobic agent in silane [25]. When the catalysts were heat treated at 500 °C under 300 ppm NH₃ gas with N₂ gas for 2h, the silane molecules underwent thermal decomposition. Subsequently, the catalyst surface acquired NH₄⁺ on their active sites. As a result, the V₂O₅-WO₃/TiO₂ catalysts were covered with NH₄⁺ layers, generating hydrophilic surface properties.

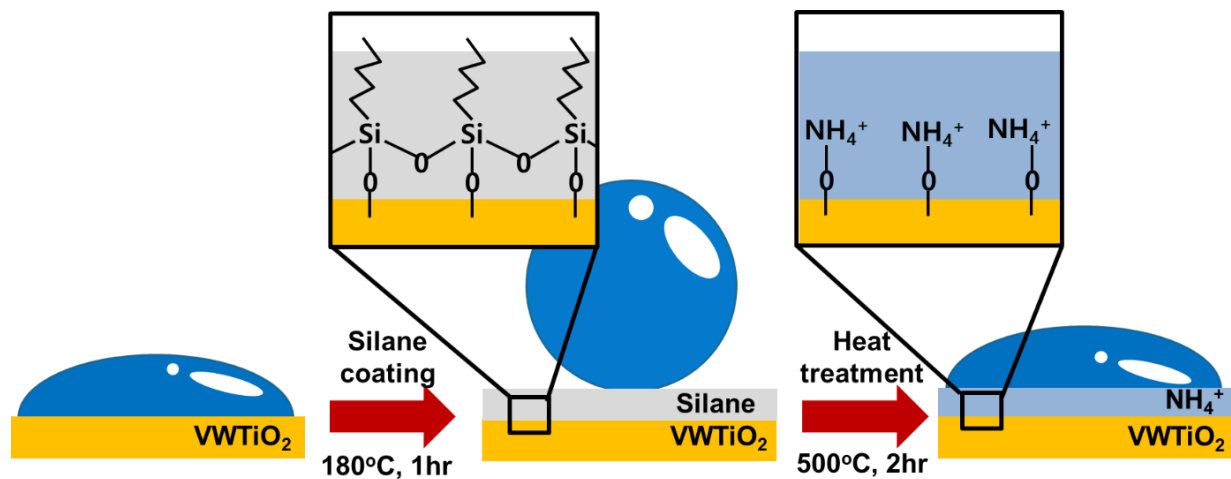


Figure 1. Schematic illustration of V_2O_5 - WO_3 / TiO_2 , silanized V_2O_5 - WO_3 / TiO_2 , and heat-treated V_2O_5 - WO_3 / TiO_2 with NH_4^+ layer coating.

The surface properties and morphology of the prepared catalysts were investigated using a scanning electron microscopy, and contact angle measurements. Figure 2a,d show the V_2O_5 - WO_3 / TiO_2 catalysts without treatment. Figure 2b,c,e,f show the results obtained for the catalyst after silane treatment and the following heat treatment, respectively. To observe the surface properties, we dropped water on the surface of the prepared SCR catalyst powders; the microscope observation results are shown in Figure 2a–c. Water that dropped on the surface was immediately absorbed into the original V_2O_5 - WO_3 / TiO_2 catalyst. The inset image shows the results of static contact angle measurement. The observed contact angle was approximately 2° , indicating that the catalysts were hydrophilic. After silane treatment of the V_2O_5 - WO_3 / TiO_2 catalyst, the water did not spread on the surface but rather formed a drop on the surface with a contact angle of approximately 160° . As the hydrophobic agent in silane covered the catalyst, the surface became hydrophobic [26]. However, the surface properties became hydrophilic after heat treating the catalyst at $500^\circ C$ for 2 h under NH_3 gas. This is because the silane molecules are thermally decomposed at a high temperature (e.g., $500^\circ C$). Subsequently, NH_3 can react to the active sites of catalyst and form NH_4^+ on the surface as a monolayer. Although the surface properties were changed by each process, the catalyst morphologies (Figure 2d–f), catalyst contents, and the textural properties (Table 1) were not changed because the prepared silane and NH_4^+ layers are quite thin.

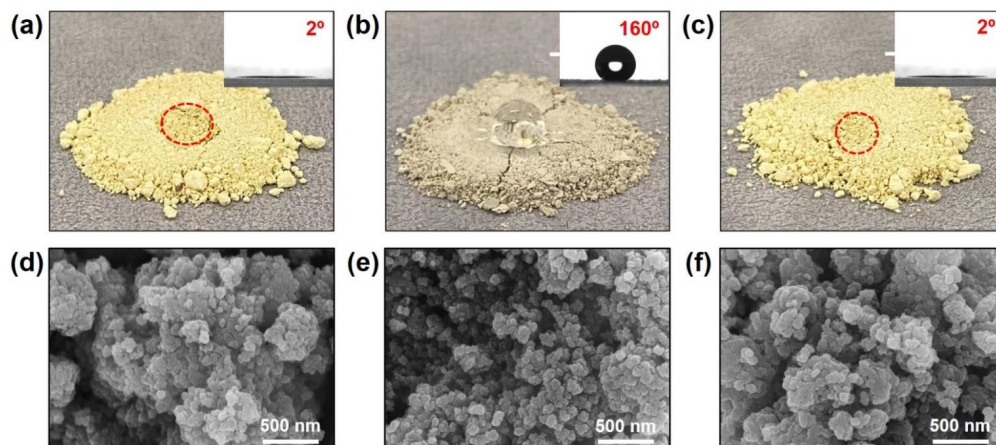


Figure 2. Microscope images of V_2O_5 - WO_3 / TiO_2 (a), silanized V_2O_5 - WO_3 / TiO_2 (b), and heat-treated V_2O_5 - WO_3 / TiO_2 (c) (insets are contact angle measurement). The red circle marks the location where the water is absorbed on the catalyst. SEM images of V_2O_5 - WO_3 / TiO_2 (d), silanized V_2O_5 - WO_3 / TiO_2 (e), and heat-treated V_2O_5 - WO_3 / TiO_2 (f).

Table 1. X-ray fluorescence analysis and Brunauer-Emmet-Teller (BET) results of the V₂O₅-WO₃/TiO₂, silanized V₂O₅-WO₃/TiO₂, and heat-treated V₂O₅-WO₃/TiO₂ catalyst.

Sample	Chemical Composition (wt.%)				S _{BET} (m ² /g)	Pore Volume (cm ³ /g)	Pore Size (nm)
	TiO ₂	V ₂ O ₅	WO ₃	SO ₃			
VW/TiO ₂	87.53	2.03	10.04	0.40	68.86	0.28	15.94
Silanized VW/TiO ₂	87.32	2.05	10.02	0.61	65.54	0.21	12.95
Heat-treated VW/TiO ₂	87.53	1.98	9.99	0.50	66.39	0.24	14.17

The crystalline structures of the prepared catalysts were determined using XRD (Figure 3a), which clearly showed anatase TiO₂, whereas peaks for V₂O₅ and WO₃ were not observed in any samples. This is because the V₂O₅ and WO₃ catalysts with small nanoparticle sizes were uniformly coated on the TiO₂ support, and the peaks of the V₂O₅ and WO₃ catalysts were hard to detect using XRD [27]. Furthermore, the peak intensities and positions were similar for all catalysts, indicating that silane and heat treatments under NH₃ gas did not affect the crystallinity of the V₂O₅-WO₃/TiO₂ catalyst.

To observe the silane layer and difference in chemical bonding in the catalyst after the heat-treatment process, XPS analysis was conducted (Figure 3b–d). Figure 3b shows the survey peaks in the XPS spectra. The XPS spectra of the Si 2p peak of the V₂O₅-WO₃/TiO₂ catalyst (black line), silanized V₂O₅-WO₃/TiO₂ catalyst (blue line), and following catalyst after heat treatment (red and green lines) are shown in Figure 3c. In the V₂O₅-WO₃/TiO₂ catalyst, no Si 2p peak was observed. After silane treatment, silicon atoms appeared at low binding energy (102 eV), indicating that silane was coated on the V₂O₅-WO₃/TiO₂ catalyst. However, the peaks at 102 eV disappeared after heat treatment of the silanized V₂O₅-WO₃/TiO₂ catalyst, indicating that the coated silane had decomposed at temperatures over 500 °C. By contrast, binding energies near 401 and 399 eV were observed for the heat-treated V₂O₅-WO₃/TiO₂ catalyst (Figure 3d). The intensity of V₂O₅-WO₃/TiO₂ catalyst and silanized V₂O₅-WO₃/TiO₂ catalyst were lower, but the intensity was larger for the heat-treated V₂O₅-WO₃/TiO₂ catalyst. The binding energies were attributed to the neutral amine's residual on the surface and NH₄⁺, respectively, from the flowing NH₃ gas during the heat-treatment process [28,29]. The NH₂ peak at around 399 eV came from the use of ammonium-based precursors of V and W, and the NH₂ peak is observed in all samples. Table 2 and S1 show the atomic contents of the prepared catalysts obtained from XPS spectra. Heat-treated V₂O₅-WO₃/TiO₂ catalyst had increased N concentration of 0.79 at.% compared with the V₂O₅-WO₃/TiO₂ catalyst (0.40 at.%) and the Silanized V₂O₅-WO₃/TiO₂ catalyst (0.31 at.%). The results indicate that the NH₄⁺ layer is formed on the heat-treated V₂O₅-WO₃/TiO₂ catalyst.

Table 2. Atomic percent of element obtained from XPS spectra of the V₂O₅-WO₃/TiO₂, silanized V₂O₅-WO₃/TiO₂, heat-treated V₂O₅-WO₃/TiO₂ catalyst.

Sample	Element (at.%)								
	N	O	Si	F	C	S	V	W	Ti
VW/TiO ₂	0.40	52.47	-	-	18.28	0.53	1.55	1.82	24.95
Silanized VW/TiO ₂	0.31	45.90	0.24	12.89	19.91	0.24	1.28	1.36	17.89
Heat-treated VW/TiO ₂	0.79	56.44	-	-	18.06	0.61	1.34	1.80	20.96

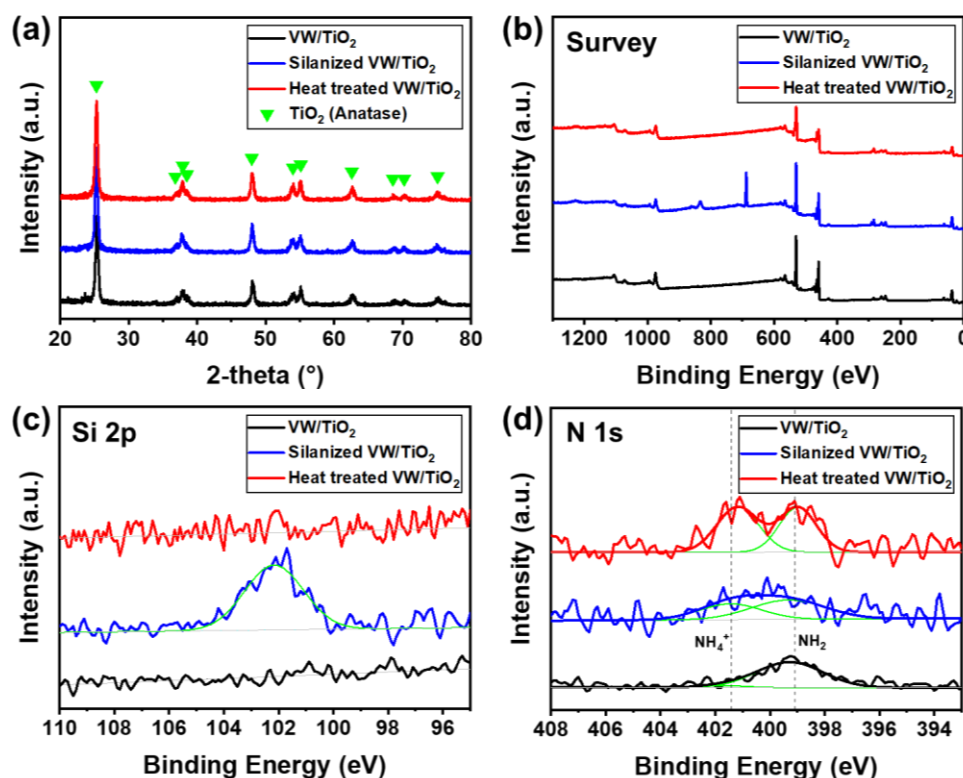


Figure 3. (a) XRD patterns and XPS spectra for (b) survey, (c) Si 2p, and (d) N 1s of V_2O_5 - WO_3 / TiO_2 (black line), silanized V_2O_5 - WO_3 / TiO_2 (blue line), and heat-treated V_2O_5 - WO_3 / TiO_2 (red line).

The NO_x removal efficiency and N_2 selectivity following the formation of the NH_4^+ layer on the surface of the V_2O_5 - WO_3 / TiO_2 catalyst were measured in a fixed bed (Figure 4). Figure 4a shows the NO_x removal efficiency of the prepared samples, which were higher for the silanized catalyst and heated silanized catalyst than for the original V_2O_5 - WO_3 / TiO_2 catalyst below 300 °C. The catalytic performance of the silanized V_2O_5 - WO_3 / TiO_2 catalyst improved from 45% to 60%, particularly at 200 °C. Figure 4b shows the N_2 selectivity; a trace amount of N_2O in the prepared catalyst was produced at 300 °C. The trend in N_2 selectivity was similar to the NO_x removal efficiency, and the heat-treated V_2O_5 - WO_3 / TiO_2 catalyst showed a higher N_2 selectivity at 420 °C. Sulfur in the fuel deactivated the catalyst through the poisoning effect, specifically in the low-temperature range (below 300 °C). When vanadium catalysts are exposed to SO_x , ammonium bisulfate (NH_4HSO_4) and ammonium sulfate ($(NH_4)_2SO_4$) are formed on the catalyst surface, decreasing efficiency [24]. The hydrophobic properties of the coated silane prevent the formation of ammonium sulfate on the V_2O_5 - WO_3 / TiO_2 catalyst surface, enhancing the NO_x removal efficiency at low temperatures. Interestingly, the NO_x removal efficiency of the silanized catalyst after heat treatment was higher than that of the silanized and original catalysts. The NH_4^+ intermediates in the catalyst exhibit high catalytic activity and proton conductivity in NH_3 SCR, particularly in the low-temperature range. Therefore, the NH_4^+ layer on the catalyst produced by silane and heat treatments leads to enhanced NO_x removal efficiency at low temperatures, specifically at 250 °C, because of the higher proton conductivity and reactivity [30], whereas silane is decomposed and reacts with NH_3 at over 300 °C in the reaction gas during fixed bed evaluation, and some NH_4^+ is produced on the catalyst surface. Therefore, the silanized and heat-treated V_2O_5 - WO_3 / TiO_2 catalysts show similar catalytic performances at high temperatures (>300 °C). Note that there was no significant difference in the NO_x removal efficiency and N_2 selectivity between V_2O_5 - WO_3 / TiO_2 and heat-treated V_2O_5 - WO_3 / TiO_2 without a silane coating process in the temperature range of 150–420 °C (Figure S1). This results demonstrate that silane coating is a key process to prepare ammonium ion enhanced V_2O_5 - WO_3 / TiO_2 catalysts.

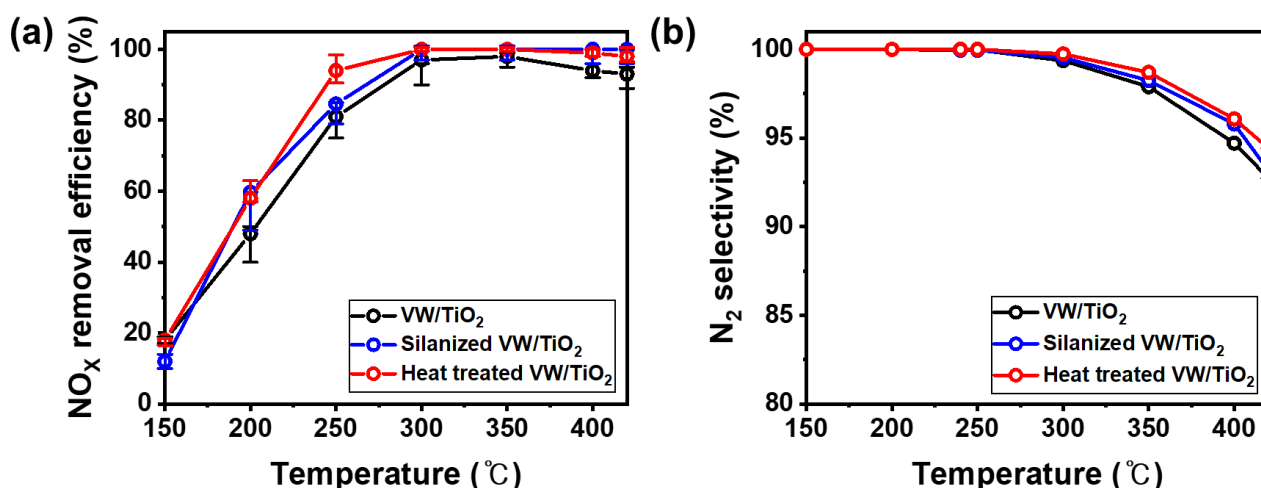


Figure 4. NO_x removal efficiency (a) and N₂ selectivity (b) of V₂O₅-WO₃/TiO₂ (black line), silanized V₂O₅-WO₃/TiO₂ (blue line), and heat-treated V₂O₅-WO₃/TiO₂ (red line). Reaction conditions: [NO] = 300 ppm, [NH₃] = 300 ppm, [SO₂] = 600 ppm, [O₂] = 5 vol.%, and [gas hourly space velocity] = 60,000 h⁻¹.

The formed NH₄⁺ layer and acid sites were analyzed using FT-IR spectra, as shown in Figure 5a–c. Si-CH₂ and Si-O-Si bond peaks only appeared at 1250 and 1216 cm⁻¹, respectively, in the silanized V₂O₅-WO₃/TiO₂ catalyst (Figure 5b). After heat treatment, the peaks related to Si (e.g., 1250 and 1216 cm⁻¹) disappeared while various peaks related to NH₄⁺ started to appear in the range of 1400 to 1600 cm⁻¹. Furthermore, the peak near 3300 cm⁻¹ corresponds to N-H stretching (Figure 5c). According to these results, the coated silane layer disappeared during heat treatment, and a new NH₄⁺ layer was generated after the decomposition of Si atoms on the surface. To investigate the redox properties of the prepared catalysts depending on the silane treatment and formation of the NH₄⁺ layer, we analyzed the H₂-temperature-programmed reduction profiles (Figure 5d). V₂O₅-WO₃/TiO₂ exhibited three reduction peaks at 397.1 °C, 480.2 °C, and 800.8 °C, which were assigned to the reduction of V⁵⁺ to V³⁺ in the vanadium oxides, the reduction of W⁶⁺ to W⁴⁺, and the reduction of W⁴⁺ to W⁰ in the tungsten oxide, respectively [31–33]. After coating the NH₄⁺ layer on the V₂O₅-WO₃/TiO₂ catalyst surface, the reduction peaks shifted to lower temperatures of 385.6 °C, 461.2 °C, and 778.7 °C, respectively. As the NH₄⁺ layer on the surface has high proton conductivity and activity, the active materials reduced a larger amount of NO_x.

To investigate the effect of the NH₄⁺ layer under actual conditions, we applied the NH₄⁺ layer on the commercial catalyst (Figure 6). Figure 6a shows a plate-type commercial catalyst containing V₂O₅, MoO₃, TiO₂, etc. (Table S2), which is used in electric power stations to reduce NO_x gas emissions. The catalyst surface was hydrophilic, similar to the power type of the catalyst (Figure 6b). Silane treatment was conducted by the vapor evaporation method, and the surface became hydrophobic (Figure 6c). Finally, after heat treating the silanized catalysts at 500 °C for 2h under NH₃ gas with N₂ gas, the surface properties were hydrophilic because of decomposition of the silane layer and because of coating the NH₄⁺ layer on the catalyst surface (Figure 6d).

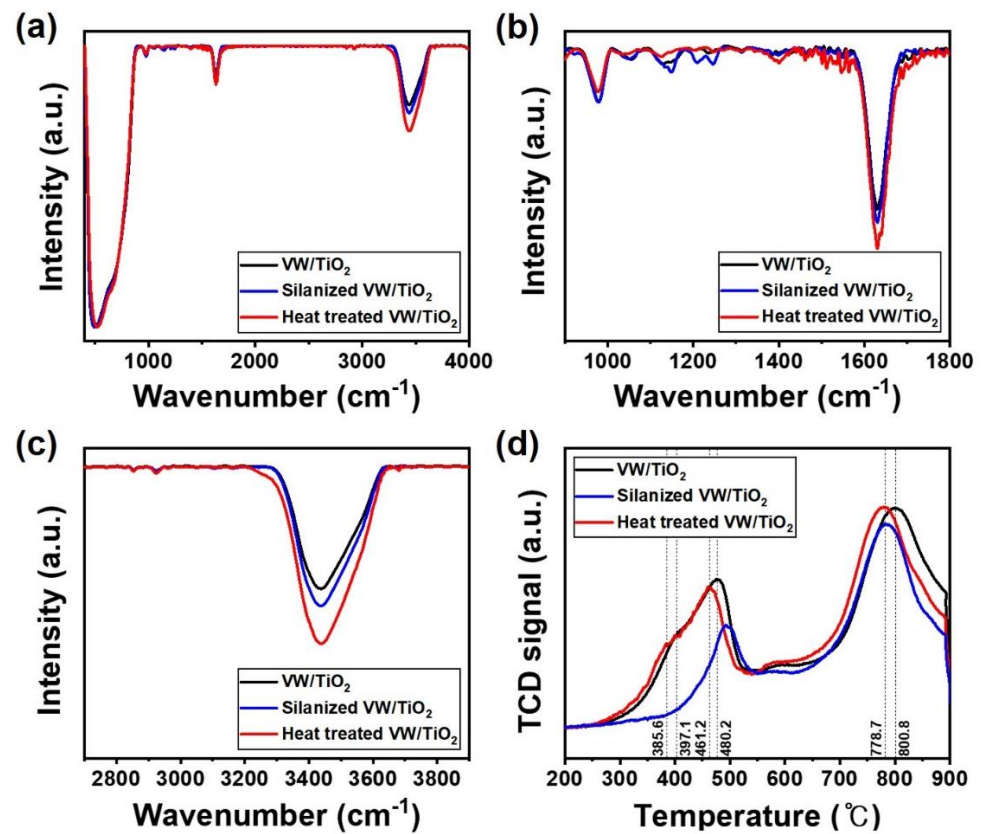


Figure 5. Fourier transform infrared spectra (a–c) and H₂-temperature-programmed reduction (d) of V₂O₅-WO₃/TiO₂ (black line), silanized V₂O₅-WO₃/TiO₂ (blue line), and heat-treated V₂O₅-WO₃/TiO₂ (red line).

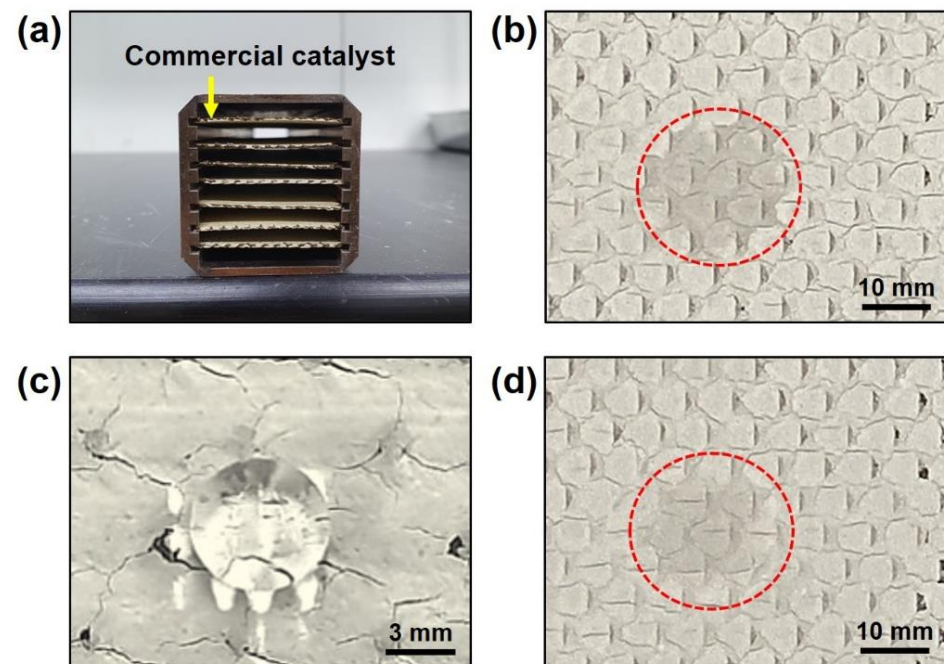


Figure 6. Microscope image of plate-type commercial catalyst (a), commercial catalyst surface (b), silanized commercial catalyst surface (c), and heat-treated commercial catalyst surface (d) after dropping water.

The prepared plate-type commercial catalysts were evaluated in a microreactor from 200 °C to 450 °C, as shown in Figure 7. The commercial catalysts exhibited a lower NO_x removal efficiency at 200 °C, which gradually increased to 400 °C. The commercial catalyst specialized in high temperature range over 300 °C because it used an electric power plant. Therefore, the NO_x removal efficiency is not largely changed at high temperature. After forming the NH₄⁺ layer on the catalyst, the NO_x removal efficiency was enhanced over a wide window range from 200 °C to 450 °C, particularly at 200 °C. Usually, the catalytic efficiency deteriorated at lower temperature due to generating ammonium sulfate on the catalyst surface. However, the formed NH₄⁺ layer has high proton conductivity, which leads to the reduction of vanadium oxides and tungsten oxide, and improved the NO_x removal efficiency.

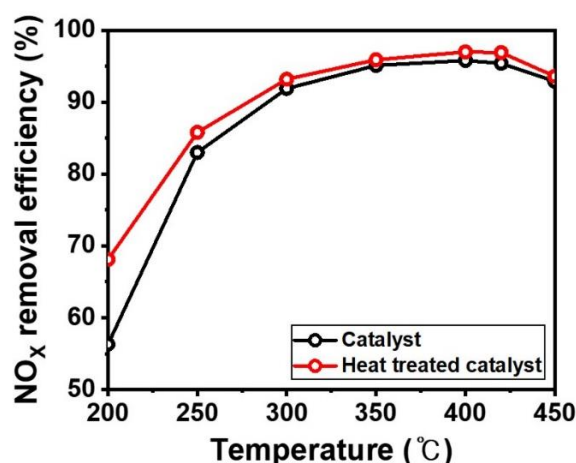


Figure 7. NO_x removal efficiency of V₂O₅-WO₃/TiO₂ (black line) and heat-treated V₂O₅-WO₃/TiO₂ (red line). Reaction conditions: [NO] = 240 ppm [NH₃] = 288 ppm, [SO₂] = 600 ppm, [O₂] = 3 vol.%, [area velocity] = 25 m/h.

4. Conclusions

We investigated the effect of coating of V₂O₅-WO₃/TiO₂ catalysts with an NH₄⁺ layer through heat treatment of silanized catalysts at 500 °C under NH₃ gas with N₂ gas. The silane molecules were substituted with NH₄⁺ by decomposing the silane layer on the surface. V₂O₅-WO₃/TiO₂ catalysts with an NH₄⁺ layer showed an increased NO_x removal efficiency over a wide temperature range (150–420 °C) compared with the V₂O₅-WO₃/TiO₂ catalysts. Particularly, the performance was improved at low temperatures (<300 °C). The coated NH₄⁺ layer led to enhanced proton conductivity and promoted further reduction of vanadium oxides and tungsten oxide. The V₂O₅-WO₃/TiO₂ catalysts with an NH₄⁺ layer exhibited improved SCR performance. These results may contribute to future studies on SCR catalysts and other catalyst systems.

Supplementary Materials: The following are available online at <https://www.mdpi.com/article/10.3390/nano11102677/s1>, Figure S1: NO_x removal efficiency (a) and N₂ selectivity (b) of V₂O₅-WO₃/TiO₂ (black line) and heat-treated V₂O₅-WO₃/TiO₂ without the silane coating process (red line). Reaction conditions: [NO] = 300 ppm, [NH₃] = 300 ppm, [SO₂] = 600 ppm, [O₂] = 5 vol.%, and GHSV = 60,000 h⁻¹., Table S1: Atomic percent of elements obtained from the XPS spectra of the heat-treated V₂O₅-WO₃/TiO₂ catalyst without silane coating process., Table S2: X-ray fluorescence analysis of the commercial plate-type monoliths.

Author Contributions: Conceptualization, G.K. and D.H.L.; methodology, B.J., J.-W.P., and T.K.; validation, J.-W.L.; writing—original draft preparation, M.S.L. and S.-I.K.; writing—review and editing, G.K. and D.H.L.; project administration, D.H.L. All authors have read and agreed to the published version of the manuscript.

Funding: D.H.L. was supported by the Korea Institute of Industrial Technology (KITECH), (grant number IZ200073) and the Ministry of Trade, Industry, and Energy, South Korea (MOTIE) (grant number 20005721). G.K. was supported by Hanwha Solution Corporation (grant number 43041).

Institutional Review Board Statement: Not applicable.

Informed Consent Statement: Not applicable.

Data Availability Statement: The data are contained within the article.

Conflicts of Interest: The authors declare no conflict of interest.

References

1. Damma, D.; Ettireddy, P.R.; Reddy, B.M.; Smirniotis, P.G. A review of low temperature NH₃-SCR for removal of NO_x. *Catalysts* **2019**, *9*, 349. [[CrossRef](#)]
2. Lee, M.J.; Kim, D.H.; Lee, M.; Ye, B.; Jeong, B.; Lee, D.; Kim, H.D.; Lee, H. Enhanced NO_x removal efficiency for SCR catalyst of well-dispersed Mn-Ce nanoparticles on hexagonal boron nitride. *Environ. Sci. Pollut. Res.* **2019**, *26*, 36107–36116. [[CrossRef](#)]
3. Zhang, S.; Zhang, B.; Liu, B.; Sun, S. A review of Mn-containing oxide catalysts for low temperature selective catalytic reduction of NO_x with NH₃: Reaction mechanism and catalyst deactivation. *RSC Adv.* **2017**, *7*, 26226–26242. [[CrossRef](#)]
4. Fu, M.; Li, C.; Lu, P.; Qu, L.; Zhang, M.; Zhou, Y.; Yu, M.; Fang, Y. A review on selective catalytic reduction of NO_x by supported catalysts at 100–300 C—catalysts, mechanism, kinetics. *Catal. Sci. Technol.* **2014**, *4*, 14–25. [[CrossRef](#)]
5. Ye, B.; Lee, M.; Jeong, B.; Kim, J.; Lee, D.H.; Baik, J.M.; Kim, H.D. Partially reduced graphene oxide as a support of Mn-Ce/TiO₂ catalyst for selective catalytic reduction of NO_x with NH₃. *Catal. Today* **2019**, *328*, 300–306. [[CrossRef](#)]
6. Lee, M.S.; Kim, S.I.; Lee, M.J.; Ye, B.; Kim, T.; Kim, H.D.; Lee, J.W.; Lee, D.H. Effect of Catalyst Crystallinity on V-Based Selective Catalytic Reduction with Ammonia. *Nanomaterials* **2021**, *11*, 1452. [[CrossRef](#)]
7. Zhang, X.; Diao, Q.; Hu, X.; Wu, X.; Xiao, K.; Wang, J. Modification of V₂O₅-WO₃/TiO₂ Catalyst by Loading of MnO_x for Enhanced Low-Temperature NH₃-SCR Performance. *Nanomaterials* **2020**, *10*, 1900. [[CrossRef](#)] [[PubMed](#)]
8. Jeong, B.; Ye, B.; Kim, E.-S.; Kim, H.-D. Characteristics of selective catalytic reduction (SCR) catalyst adding graphene-tungsten nanocomposite. *Catal. Commun.* **2017**, *93*, 15–19. [[CrossRef](#)]
9. Lai, J.-K.; Wachs, I.E. A Perspective on the Selective Catalytic Reduction (SCR) of NO with NH₃ by Supported V₂O₅-WO₃/TiO₂ Catalysts. *ACS Catal.* **2018**, *8*, 6537–6551. [[CrossRef](#)]
10. Djerad, S.; Tifouti, L.; Crocoll, M.; Weisweiler, W. Effect of vanadia and tungsten loadings on the physical and chemical characteristics of V₂O₅-WO₃/TiO₂ catalysts. *J. Mol. Catal. A Chem.* **2004**, *208*, 257–265. [[CrossRef](#)]
11. Chen, J.; Peng, G.; Liang, T.; Zhang, W.; Zheng, W.; Zhao, H.; Guo, L.; Wu, X. Catalytic Performances of Cu/MCM-22 Zeolites with Different Cu loadings in NH₃-SCR. *Nanomaterials* **2020**, *10*, 2170. [[CrossRef](#)] [[PubMed](#)]
12. Li, W.; Zhang, C.; Li, X.; Tan, P.; Zhou, A.; Fang, Q.; Chen, G. Ho-modified Mn-Ce/TiO₂ for low-temperature SCR of NO_x with NH₃: Evaluation and characterization. *Chin. J. Catal.* **2018**, *39*, 1653–1663. [[CrossRef](#)]
13. Huang, J.; Huang, H.; Jiang, H.; Liu, L. The promotional role of Nd on Mn/TiO₂ catalyst for the low-temperature NH₃-SCR of NO_x. *Catal. Today* **2019**, *332*, 49–58. [[CrossRef](#)]
14. Meng, D.; Zhan, W.; Guo, Y.; Guo, Y.; Wang, L.; Lu, G. A highly effective catalyst of Sm-MnO_x for the NH₃-SCR of NO_x at low temperature: Promotional role of Sm and its catalytic performance. *ACS Catal.* **2015**, *5*, 5973–5983. [[CrossRef](#)]
15. Sun, P.; Guo, R.-T.; Liu, S.-M.; Wang, S.-X.; Pan, W.-G.; Li, M.-Y. The enhanced performance of MnO_x catalyst for NH₃-SCR reaction by the modification with Eu. *Appl. Catal. A Gen.* **2017**, *531*, 129–138. [[CrossRef](#)]
16. Kwak, J.H.; Tran, D.; Burton, S.D.; Szanyi, J.; Lee, J.H.; Peden, C.H.F. Effects of hydrothermal aging on NH₃-SCR reaction over Cu/zeolites. *J. Catal.* **2012**, *287*, 203–209. [[CrossRef](#)]
17. Guo, R.-T.; Li, M.-Y.; Sun, P.; Pan, W.-G.; Liu, S.-M.; Liu, J.; Sun, X.; Liu, S.-W. Mechanistic Investigation of the Promotion Effect of Bi Modification on the NH₃-SCR Performance of Ce/TiO₂ Catalyst. *J. Phys. Chem. C* **2017**, *121*, 27535–27545. [[CrossRef](#)]
18. Hu, H.; Xie, J.L.; Fang, D.; He, F. Study of Co-Mn/TiO₂ SCR catalyst at low temperature. In *Advanced Materials Research*; Trans Tech Publications Ltd.: Zürich, Switzerland, 2015; Volume 1102, pp. 11–16.
19. Ou, X.; Chen, K.; Wei, L.; Deng, Y.; Li, J.; Li, B.; Dong, L. Effect of Co Doping on Magnetic and CO-SCR Properties of γ-Fe₂O₃. *Ind. Eng. Chem. Res.* **2021**, *60*, 5744–5757. [[CrossRef](#)]
20. Shen, M.; Li, C.; Wang, J.; Xu, L.; Wang, W.; Wang, J. New insight into the promotion effect of Cu doped V₂O₅/WO₃-TiO₂ for low temperature NH₃-SCR performance. *RSC Adv.* **2015**, *5*, 35155–35165. [[CrossRef](#)]
21. Guo, R.T.; Sun, P.; Pan, W.G.; Li, M.Y.; Liu, S.M.; Sun, X.; Liu, S.W.; Liu, J. A Highly Effective MnNdO_x Catalyst for the Selective Catalytic Reduction of NO_x with NH₃. *Ind. Eng. Chem. Res.* **2017**, *56*, 12566–12577. [[CrossRef](#)]
22. Liu, K.; Liu, F.; Xie, L.; Shan, W.; He, H. DRIFTS study of a Ce-W mixed oxide catalyst for the selective catalytic reduction of NO_x with NH₃. *Catal. Sci. Technol.* **2015**, *5*, 2290–2299. [[CrossRef](#)]
23. Forzatti, P.; Nova, I.; Tronconi, E. New enhanced NH₃-SCR reaction for NO_x emission control. *Ind. Eng. Chem. Res.* **2010**, *49*, 10386–10391. [[CrossRef](#)]
24. Bae, Y.K.; Kim, T.-W.; Kim, J.-R.; Kim, Y.; Ha, K.-S.; Chae, H.-J. Enhanced SO₂ tolerance of V₂O₅-Sb₂O₃/TiO₂ catalyst for NO reduction with co-use of ammonia and liquid ammonium nitrate. *J. Ind. Eng. Chem.* **2021**, *96*, 277–283. [[CrossRef](#)]

25. Kobaku, S.P.R.; Kota, A.K.; Lee, D.H.; Mabry, J.M.; Tuteja, A. Patterned Superomniphobic-Superomniphilic Surfaces: Templates for Site-Selective Self-Assembly. *Angew. Chem.* **2012**, *124*, 10256–10260. [[CrossRef](#)]
26. Golovin, K.; Lee, D.H.; Mabry, J.M.; Tuteja, A. Transparent, Flexible, Superomniphobic Surfaces with Ultra-Low Contact Angle Hysteresis. *Angew. Chem.* **2013**, *125*, 13245–13249. [[CrossRef](#)]
27. Li, S.; Huang, W.; Xu, H.; Chen, T.; Ke, Y.; Qu, Z.; Yan, N. Alkali-induced deactivation mechanism of V₂O₅-WO₃/TiO₂ catalyst during selective catalytic reduction of NO by NH₃ in aluminum hydrate calcining flue gas. *Appl. Catal. B Environ.* **2020**, *270*, 118872. [[CrossRef](#)]
28. Kang, H.; Hong, S.; Lee, J.; Lee, K. Electrostatically Self-Assembled Nonconjugated Polyelectrolytes as an Ideal Interfacial Layer for Inverted Polymer Solar Cells. *Adv. Mater.* **2012**, *24*, 3005–3009. [[CrossRef](#)]
29. Liu, G.; Tao, C.; Zhang, M.; Gu, X.; Meng, F.; Zhang, X.; Chen, Y.; Ruan, S. Effects of surface self-assembled NH₄⁺ on the performance of TiO₂-based ultraviolet photodetectors. *J. Alloy. Compd.* **2014**, *601*, 104–107. [[CrossRef](#)]
30. Chen, P.; Jabłońska, M.; Weide, P.; Caumanns, T.; Weirich, T.E.; Muhler, M.; Moos, R.; Palkovits, R.; Simon, U. Formation and Effect of NH₄⁺ Intermediates in NH₃-SCR over Fe-ZSM-5 Zeolite Catalysts. *ACS Catal.* **2016**, *6*, 7696–7700. [[CrossRef](#)]
31. Zhang, Y.; Guo, W.; Wang, L.; Song, M.; Yang, L.; Shen, K.; Xu, H.; Zhou, C. Characterization and activity of V₂O₅-CeO₂/TiO₂-ZrO₂ catalysts for NH₃-selective catalytic reduction of NO_x. *Chin. J. Catal.* **2015**, *36*, 1701–1710. [[CrossRef](#)]
32. Wu, X.; Yu, W.; Si, Z.; Weng, D. Chemical deactivation of V₂O₅-WO₃/TiO₂ SCR catalyst by combined effect of potassium and chloride. *Front. Environ. Sci. Eng.* **2013**, *7*, 420–427. [[CrossRef](#)]
33. Lee, M.; Ye, B.; Jeong, B.; Chun, H.-Y.; Lee, D.H.; Park, S.-S.; Lee, H.; Kim, H.-D. Reduced graphene oxide supported V₂O₅-WO₃-TiO₂ catalysts for selective catalytic reduction of NO_x. *Korean J. Chem. Eng.* **2018**, *35*, 1988–1993. [[CrossRef](#)]